# Co-aggregate formation of CADASIL-mutant NOTCH3: a single-particle analysis

Marco Duering<sup>1,†</sup>, Anna Karpinska<sup>1,†</sup>, Stefanie Rosner<sup>1</sup>, Franziska Hopfner<sup>1</sup>, Martin Zechmeister<sup>1</sup>, Nils Peters<sup>2</sup>, Elisabeth Kremmer<sup>4</sup>, Christof Haffner<sup>1</sup>, Armin Giese<sup>3,‡</sup>, Martin Dichgans<sup>1,‡</sup> and Christian Opherk<sup>1,2,\*,‡</sup>

<sup>1</sup>Institute for Stroke and Dementia Research, <sup>2</sup>Department of Neurology, <sup>3</sup>Department of Neuropathology, Ludwig-Maximilians-University, 81377 Munich, Germany and <sup>4</sup>Institute of Molecular Immunology, Helmholtz Center, 81377 Munich, Germany

Received March 16, 2011; Revised April 27, 2011; Accepted May 22, 2011

CADASIL (cerebral autosomal dominant arteriopathy with subcortical infarcts and leukoencephalopathy) is the most common monogenic cause of stroke and vascular dementia. Accumulation and deposition of the NOTCH3 (N3) extracellular domain in small blood vessels has been recognized as a central pathological feature of the disease. Recent experiments suggested enhanced formation of higher order multimers for mutant N3 compared with wild-type (WT). However, the mechanisms and consequences of N3 multimerization are still poorly understood, in part because of the lack of an appropriate in vitro aggregation assay. We therefore developed and validated a robust assay based on recombinant N3 fragments purified from cell culture supernatants. Using single-molecule analysis techniques such as scanning for intensely fluorescent targets and single-particle fluorescence resonance energy transfer, we show that spontaneous aggregation is limited to CADASIL-mutant N3, recapitulating a central aspect of CADASIL pathology in vitro. N3 aggregation requires no co-factor and is facilitated by sulfhydryl crosslinking. Although WT N3 does not exhibit multimerization itself, it can participate in aggregates of mutant N3. Furthermore, we demonstrate that thrombospondin-2, a known interaction partner of N3, co-aggregates with mutant N3. Sequestration of WT N3 and other proteins into aggregates represents a potentially important disease mechanism. These findings in combination with a new assay for single-molecule aggregation analysis provide novel opportunities for the development of therapeutic strategies.

#### INTRODUCTION

Cerebral small vessel disease (SVD) is a major cause of stroke and the leading cause of both silent infarcts and vascular cognitive impairment (1,2). Cerebral autosomal dominant arteriopathy with subcortical infarcts and leukoencephalopathy (CADASIL) is a hereditary SVD (3,4) caused by mutations in the *NOTCH3* gene. *NOTCH3* encodes for a large type-I transmembrane receptor (NOTCH3—N3) mainly expressed in vascular smooth muscle cells and pericytes (5).

N3 is synthesized as a 280 kDa precursor, reaches the cell surface and, after ligand binding, undergoes shedding by

ADAM proteases, thus releasing the 210 kDa N3 extracellular domain (N3-ECD). Following another cleavage event, the N3 intracellular domain (N3-ICD) is liberated from the cell membrane and translocated to the nucleus, where it regulates gene expression. The consequences of CADASIL mutations on N3 receptor function are still under debate. Previous experiments in transfected cells and transgenic mice strongly argue against a classic gain- or loss-of-function mechanism (6-9).

CADASIL-associated mutations typically affect the N3-ECD within one of the 34 epidermal growth factor (EGF)-like repeat domains. Each EGF-like repeat domain contains a highly conserved number of six cysteine residues which

<sup>\*</sup>To whom correspondence should be addressed at: Institute for Stroke and Dementia Research and Department of Neurology, Ludwig-Maximilians-University, Marchioninistr. 15, D-81377 Munich, Germany. Tel: +49 8970958315; Fax: +49 897095 8332; Email: christian.opherk@med.uni-muenchen.de 
†The authors wish it to be known that, in their opinion, the first two authors should be regarded as joint First Authors.
‡Co-corresponding authors.

seem to stabilize the domain by the formation of disulfide bonds (10). Virtually, all CADASIL mutations hitherto described result in an odd number of cysteine residues, thus leaving one residue unpaired. It has therefore been postulated that mutant N3 may interact with adjacent N3 receptors or other proteins via the unpaired cysteine sulfhydryl group (11). Indeed, accumulation and deposition of N3-ECD within vessels of affected patients represents the central hallmark of CADASIL (12). These deposits are a component of the so-called granular osmiophilic material that is CADASILpathognomonic on electron microscopy. According to recent data from transgenic mice, N3 accumulation seems to be a very early event in pathogenesis (13). Therefore, N3 multimerization has become a key target both for delineation of CADASIL pathophysiology and—as in other protein aggregation disorders—for potential therapeutic strategies. Still, the mechanisms and determinants of N3 multimerization are poorly understood.

Using a single-particle approach (scanning for intensely fluorescent targets—SIFT), we have previously shown that N3 receptors self-associate and that CADASIL mutations enhance N3 multimerization (14). However, previous experiments with N3 were impeded by the requirement to use cell lysates from N3 overexpressing cells. Thus, we could not exclude that multimerization in these experiments was related to protein overexpression and associated receptor misfolding or dependent on the presence of other proteins or cellular compounds within the lysate. These limitations precluded the use of this approach for further characterization of aggregate formation and analysis of influencing factors or conditions.

To overcome these limitations, we developed a robust assay based on recombinant N3 receptor fragments purified from cell culture supernatant. Using this natively folded protein, we show that spontaneous aggregation of N3 is limited to the CADASIL-mutant receptor, requires no co-factor and is facilitated by crosslinking of sulfhydryl groups. Furthermore, we demonstrate that wild-type (WT) N3 and thrombospondin-2 (TSP-2), a known interaction partner of N3, co-aggregates with mutant N3, providing a potential new disease mechanism.

#### **RESULTS**

#### An aggregation assay using recombinant N3-EGF<sub>1-5</sub>

Previous N3 aggregation assays were limited by the use of cell-lysate-derived protein most of which might be incorrectly folded. To overcome this limitation, we first considered purification of N3-ECD from conditioned medium of transiently transfected cells. However, secretion of N3-ECD was highly inefficient (Fig. 1B). To identify an N3 fragment that is efficiently secreted, we generated C-terminally truncated forms of N3-ECD (Fig. 1A) consisting of the signal peptide and the first 15 (N3-EGF<sub>1-15</sub>, amino acids 1–618) or the first 5 EGF-like repeat domains (N3-EGF<sub>1-5</sub>, amino acids 1–234) bearing the mutational hot spot of CADASIL (15). After transient expression in HEK293E cells, these constructs showed a distinct secretion behavior: similar to N3-ECD, N3-EGF<sub>1-15</sub> was almost completely retained inside the cell, whereas

N3-EGF<sub>1-5</sub> was found as secreted protein in the medium (Fig. 1B). Therefore, secreted N3-EGF<sub>1-5</sub> was used for subsequent analysis. Of note, beta-mercaptoethanol (bME)-resistant dimers could be found for all constructs in the cell lysates, but not for secreted N3-EGF<sub>1-5</sub>, most likely indicating aberrant folding of cell-retained N3.

Purification of N3-EGF<sub>1-5</sub> fragments by metal ion affinity chromatography resulted in a purity of >90% as determined from silver-stained protein gels (Fig. 1C). Interpretation of SIFT 2D intensity histograms is shown in Figure 1D: when mixing green or red fluorescent dye-labeled proteins, dual-color high-intensity signals represent *de novo*-formed multimers comprising both proteins. Mono-color high-intensity signals originate from preformed multimers generated prior to mixing or from *de novo* multimers formed by only one of the proteins. Preformed multimers were constantly found for all protein constructs after thawing aliquots and were eliminated from the sample through ultracentrifugation (UC) before starting an experiment in order to exclusively analyze *de novo* aggregation (Fig. 1E).

## Spontaneous multimer formation of CADASIL-mutant, but not WT N3-EGF $_{1-5}$

Previous experiments with overexpressed N3-ECD in cell lysates demonstrated spontaneous multimerization of both WT and mutant N3-ECD (14). We sought to confirm these findings for recombinant N3-EGF<sub>1-5</sub> fragments. WT and CADASIL (R133C or C183R)-mutant N3-EGF<sub>1-5</sub> were analyzed over an incubation period of 5 days at 37°C (Fig. 2A). At baseline, none of the constructs showed relevant highintensity signals, demonstrating the absence of preformed aggregates. With prolonged incubation, dual-color highintensity signals increased significantly for CADASIL-mutant protein fragments, indicating formation of de novo multimers. Quantification confirmed a time-dependent increase for mutant constructs but not for WT (Fig. 2B). Turning off the red laser eliminates direct excitation of the red fluorescent dye. However, under this condition, multimers from mutant protein still emitted signals from red fluorescent dyes (Fig. 2C). In these multimers, red fluorophores are excited by fluorescence resonance energy transfer (FRET) from green fluorophores, which are are excited by the 488 nm laser. FRET at the single-particle level strongly suggests close proximity of fluorophores in dual-color multimers derived from mutant N3-EGF<sub>1-5</sub> (16).

# Validation of SIFT analysis: $N3\text{-}EGF_{1-5}$ multimers protein gel electrophoresis

To validate findings from SIFT experiments, we conducted polyacrylamdide gel electrophoresis (PAGE) and western blot analyses of spontaneous multimer formation. Consistent with SIFT experiments, mutant but not WT proteins showed a shift towards higher molecular weight complexes with prolonged incubation time under non-reducing conditions (-bME) (Fig. 3A). Starting on day 1, immunoreactive material was detected in the stacking gel, whereas signals from monomers of mutant constructs decreased over time. In contrast, WT proteins showed no significant multimer

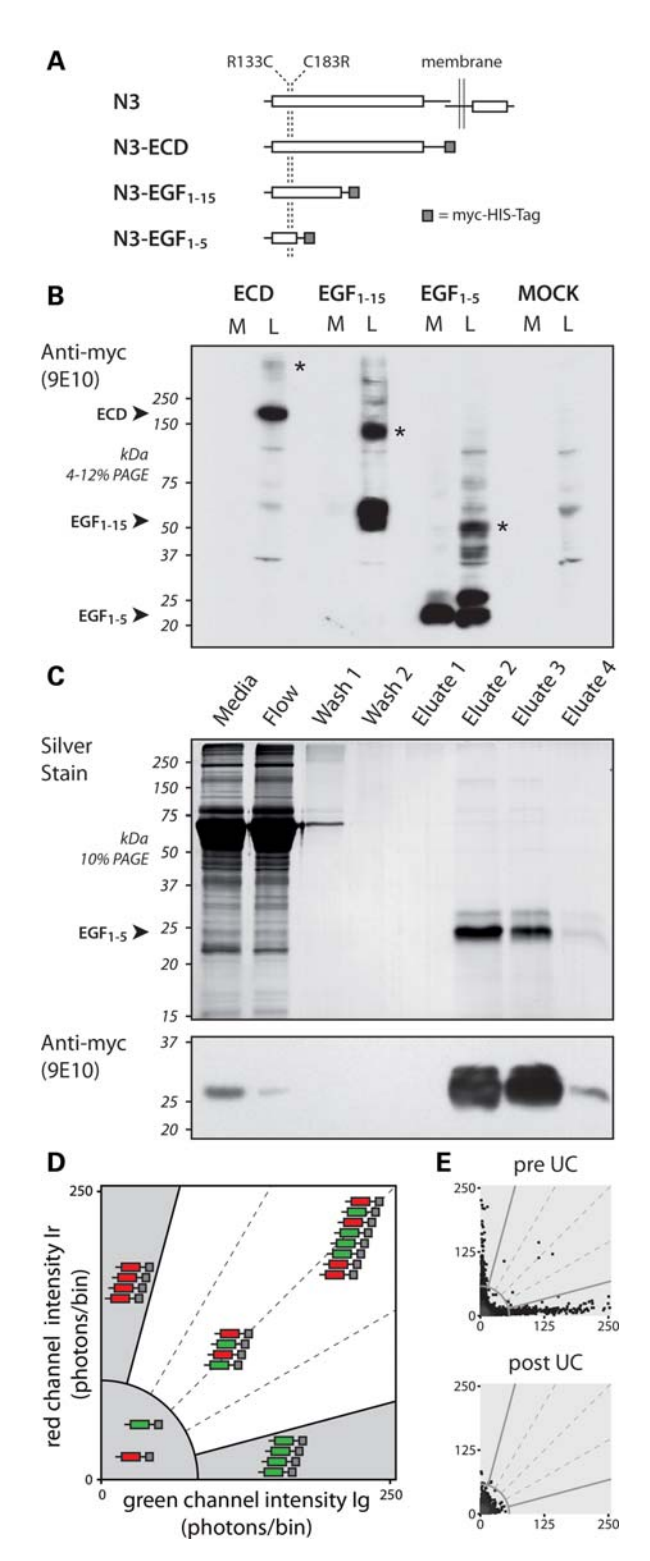


**Figure 1.** Expression and purification of N3-EGF $_{1-5}$ . (A) Schematic illustration of protein constructs used in this study. Dotted lines indicate the location of the mutations R133C and C183R. (B) Amount of secreted protein from N3 fragments (all WT) determined by PAGE and western blotting of conditioned medium (M) and cell lysate (L, adjusted to the same volume as medium) under reducing conditions. Of note, bME-resistant dimers (\*) were observed for all constructs in the lysates, but not for secreted N3-EGF $_{1-5}$ , most likely indicating aberrant folding of cell-retained N3 (MOCK, empty vector transfected). (C) Silver-stained PAGE and western blot of a representative purification of WT N3-EGF $_{1-5}$  from conditioned

formation and monomer signals were detected throughout all time points. Under reducing conditions (+bME), only monomer bands were visible, suggesting that multimers can be dissolved by treatment with sodium dodecyl sulfate (SDS) and bME. When analyzing the reversibility of multimer formation by SIFT addition of SDS or bME alone had little effect on high-intensity signals (Fig. 3B). However, when treating multimers with both SDS and bME (resembling SDS-PAGE under reducing conditions), the multimer signal was lost entirely. Consistent with these findings, solubilization of N3-ECD from CADASIL brains depends on the presence of both SDS and bME in the extraction buffer (Fig. 3C).

### Aggregation of N3-EGF $_{1-5}$ is accelerated by crosslinking of sulfhydryl groups

Almost all disease-related mutations in CADASIL involve cysteine residues within the N3-ECD. To examine the role of cysteine residues in de novo multimer formation of  $N3-EGF_{1-5}$ , we applied bismaleimide, a crosslinker highly specific for sulfhydryl groups. Bismaleimide has been successfully used to characterize oligomerization of several other proteins (17,18). With increasing concentrations of bismaleimide, there was a massive increase in the dual-color high-intensity signals already after 1 h of incubation (Fig. 4A and Supplementary Material, Fig. S1). Multimer signals of both CADASIL-mutants were significantly higher compared with WT at bismaleimide concentrations of  $>4 \mu mol/l$  (Fig. 4A). There was no significant difference between the two mutant constructs. Close proximity of the protein fragments within aggregates-as indicated by FRET-was observed for mutant constructs only. Although some multimers were seen from WT fragments at high bismaleimide concentrations, they did not show FRET (Fig. 4B). Denaturation by acidic pH served as a positive control condition for FRET detection: FRET was present for multimers of all constructs with nearly identical efficiency (Fig. 4C, Supplementary Material, Fig. S2).

To further investigate the involvement of cysteine residues, we used homocysteine, a disulfide bond-reshuffling reagent (19). The multimer signal was detected with increasing homocysteine concentration (Supplementary Material, Fig. S3A) for all constructs with no significant difference between WT and mutant protein fragments. Turning off the red excitation laser resulted in complete loss of dual-color signals, demonstrating the absence of FRET in these multimers (Fig. 4D, Supplementary Material, Fig. S3B). This suggests a different

medium (flow, column flow through). (**D**) SIFT visualization: axes in the 2D histogram represent the intensity of photon counts per bin in the detector channel (green channel along the x-axis, red along the y-axis). Monomers result in data points in the lower left corner. Multimers exhibit high-intensity signals: aggregates of one protein appear as mono-colored multimers along the axes, whereas de novo multimers from both proteins bear both fluorescent dyes and can therefore be detected in the middle sectors. For quantification, dual-color bins within this area and above the monomer threshold were counted (white area). (**E**) SIFT analysis of thawed protein (representative measurement using WT protein) shows mono-colored preformed multimers (upper panel) which were eliminated by UC before each experiment (lower panel). The measurements illustrate typical threshold and sector setups.

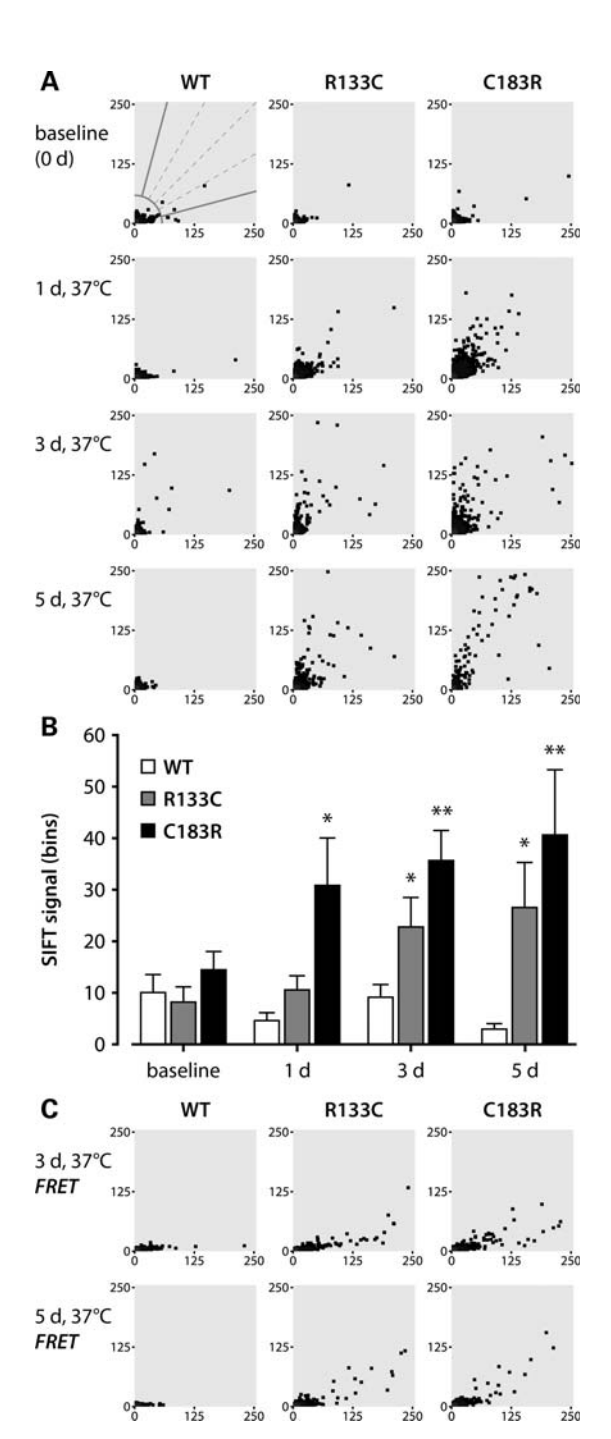


**Figure 2.** Spontaneous multimerization of CADASIL-mutant N3-EGF<sub>1-5</sub>. (A) SIFT reveals dual-color high-intensity signals after incubation for CADASIL-mutant constructs indicating spontaneous *de novo* multimer formation. Threshold and sectors for all measurements are illustrated at WT baseline. (B) Quantification of dual-color high-intensity signals. Mean + SEM of nine independent experiments (group statistics compared with WT at the same time point;  ${}^*P < 0.05$ ;  ${}^{**}P < 0.01$ ; two-tailed Mann–Whitney test). Note that WT signals decreased slightly over time, accompanied by declining diffusion time of the monomer in autocorrelation analysis (data not shown), indicating smaller protein sizes as a sign for protein degradation. (C) Single-particle FRET is only present in multimers from mutant protein fragments: although the laser exciting the red fluorescent dye is turned off, the fluorescence signal from the red dye in mutant multimers is still detected due to indirect excitation by FRET from green dyes in close proximity.

conformation compared with spontaneously or bismaleimide-induced multimers.

### CADASIL-mutant N3 co-aggregates with WT N3 and TSP-2

Because of the dominant inheritance of CADASIL, WT and mutant proteins usually co-exist in vivo. Previous co-immunoprecipitation experiments from cell lysates suggest that WT and mutant N3-ECD can interact with each other (14). However, under the conditions in these experiments, the interaction might be due to incorrectly folded N3 and thus physiologically irrelevant. Using secreted (and therefore most likely correctly folded) N3 fragments, we were able to re-examine a possible interaction under more native conditions. For this purpose, we extended our incubation experiments by mixing WT and mutant N3-EGF<sub>1-5</sub> labeled with different fluorescent dyes. After incubation at 37°C for 3 days, multimer formation was present in all samples except the mixture of green- and red-labeled WT proteins (Fig. 5A). Mixtures of WT and mutant proteins showed dualcolor high-intensity signals, representing de novo aggregates. Consistent throughout multiple experiments, the color of the mutant protein was dominant within these multimers, demonstrating that more mutant than WT molecules were incorporated. FRET was detectable for mixtures of any of the two mutant proteins or for a mixture of green WT and red mutants (data not shown).

In addition, we looked into co-aggregation of mutant N3 with recombinant TSP-2, a known interaction partner of N3 (20). The dual-color SIFT signals were detected from a of green-labeled TSP-2 and red-labeled mixture C183R-mutant N3 after incubation at 37°C for 3 days (Fig. 5B). To confirm the specificity of this finding, we conducted control experiments using alpha-synuclein. Alphasynuclein spontaneously formed multimers in a similar manner as N3 (Fig. 5B, lower right panel). However, a mixture of alpha-synuclein and mutant N3 revealed no relevant dual-color high-intensity signals after incubation (Fig. 5B, lower left panel). Instead, two mono-colored signal clusters could be detected, representing separate multimer formation without co-aggregation. In a mixture of alphasynuclein and TSP-2, strong mono-colored SIFT signals could be detected for alpha-synuclein (red), whereas TSP-2 showed only sparse multimer signals (green) (Fig. 5B, lower middle panel). No dual-color SIFT signals, representing co-aggregation, could be detected for this mixture.

#### **DISCUSSION**

Accumulation and deposition of the N3-ECD within vessel walls has been recognized as a key pathological feature in CADASIL (12). However, the connection between N3 aggregation and vessel dysfunction is poorly understood, in part because of the lack of an appropriate *in vitro* aggregation assay. Using a recombinant N3 fragment bearing the mutational hot spot of CADASIL, we developed a robust N3 aggregation assay with single-particle sensitivity and show that (i)

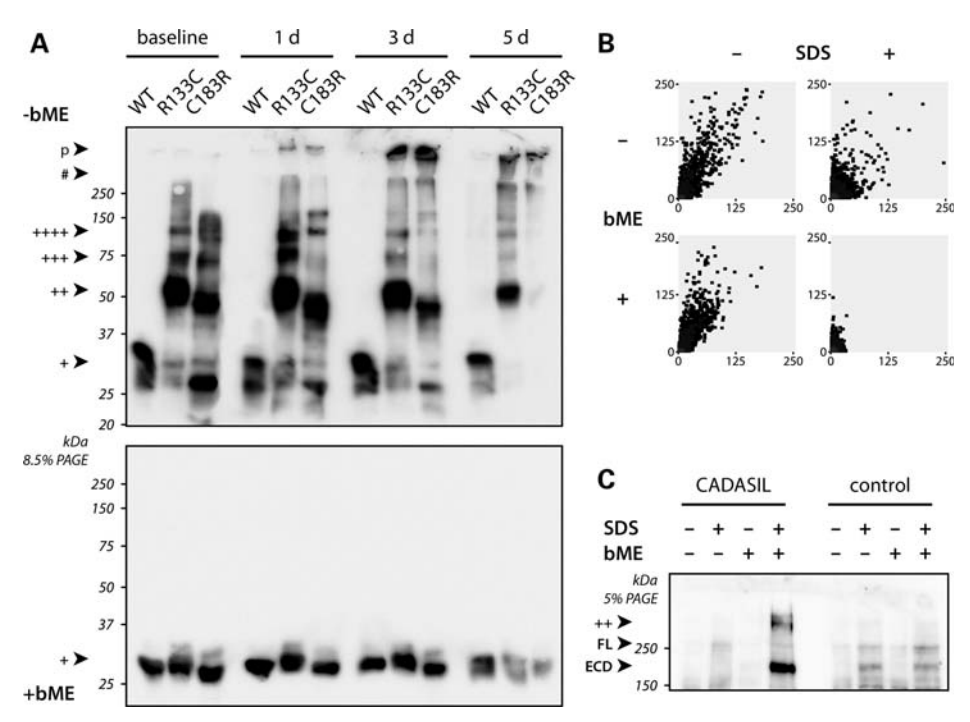


**Figure 3.** Characterization of N3-EGF $_{1-5}$  multimers. (**A**) Detection of N3-EGF $_{1-5}$  multimers by western blot using monoclonal anti-myc antibody 9E10. PAGE under non-reducing (-bME) or reducing (+bME) conditions after incubation at 37°C. Note the appearance of higher molecular weight bands and signals within the stacking gel exclusively for mutant proteins. At day 5, the majority of aggregated C183R mutant protein is apparently not entering the gel under non-reducing conditions (+, monomer; ++, dimer; ++++, trimer; ++++, tetramer; p, sample pocket; #, interface between stacking gel and resolving gel). Note the different mobility of protein fragments most likely due to different conformation and glycosylation. (**B**) Dissolving of spontaneously formed multimers from C183R-mutant protein: in agreement with western blot analysis, only the combination of SDS (1%) and bME (1%) is able to dissolve multimers (in SIFT, represented by bicolored high-intensity signals) that were spontaneously formed through incubation at 37°C for 3 days. (**C**) Solubilization of N3-ECD from CADASIL brains depends on the presence of both SDS and bME. Brain extracts were prepared in the presence or absence of SDS and bME and analyzed by protein electrophoresis using Tris-HCl buffer and gels, and western blot using monoclonal anti-N3 antibody 3G6 (++, dimer). N3-ECD and full length (FL) N3 can be detected in all fractions containing SDS. Accumulation of N3 in brains from CADASIL patients leads to enhanced signals from N3-ECD and presence of a dimer (++) only in the fraction with SDS and bME (1% v/v each).

spontaneous multimerization is limited to CADASIL-mutant N3 when working with correctly folded protein; (ii) no co-factor is needed for N3 multimerization; (iii) multimerization can be significantly enhanced by crosslinking of sulfhydryl groups; and (iv) both WT N3 and TSP-2 can co-aggregate with mutant N3.

The described assay is a significant improvement over the previous approach in which cell lysates and indirect labeling of N3 with antibodies had been used for interaction studies. These experiments showed that multimerization was enhanced, but not limited to CADASIL-mutant N3 (14). In the current setup utilizing purified protein from cell supernatant, recombinant WT protein showed no spontaneous multimer formation. This suggests a qualitative difference between the aggregation behavior of WT and that of mutant N3. The most likely explanation for the discrepancy to previous experiments is that the use of cell lysates introduced a background of disease-unrelated multimerization from incorrectly folded protein. In accordance with this, we show formation of bME-resistant dimers for all WT N3 fragments in cell lysates, whereas these dimers are absent for secreted  $N3-EGF_{1-5}$  protein in the cell supernatant (Fig. 1B). The complex folding process of the cysteine-rich EGF-like repeat domains may overburden the cellular folding machinery when overexpressing larger N3 constructs, leading to the

retention of incorrectly folded protein inside the cell. Fully in line with our observation, retention of larger N3 constructs has been observed frequently in previous studies even at lower expression levels in stably transfected cells (21,22). Our results strongly argue for the need of correctly folded protein when examining N3 aggregation.

The use of purified protein offers additional benefits: direct labeling with covalently bound fluorescent dye eliminates the need of antibodies to detect the multimers, thereby reducing potential background from unspecific antibody binding or antibody conglomerates as seen in previous experiments (14). Moreover and more importantly, due to the high purity of our protein fragment, we can conclude that essentially no co-factor is needed for mutant N3 multimerization.

The highly stereotyped nature of N3 mutations in CADASIL suggests a role of free cysteine residues in disease pathogenesis (11). Fully in line with this hypothesis, we found that the use of a sulfhydryl-specific crosslinker greatly facilitates the formation of FRET-positive multimers solely for mutant N3. Unbound cysteines might therefore represent a target for therapeutic approaches. In contrast, mere unspecific disulfide bond reshuffling by homocysteine led to the formation of N3 multimers independent of CADASIL mutations. On the one hand, this finding emphasizes the importance of disulfide bonds in N3 conformation. On the

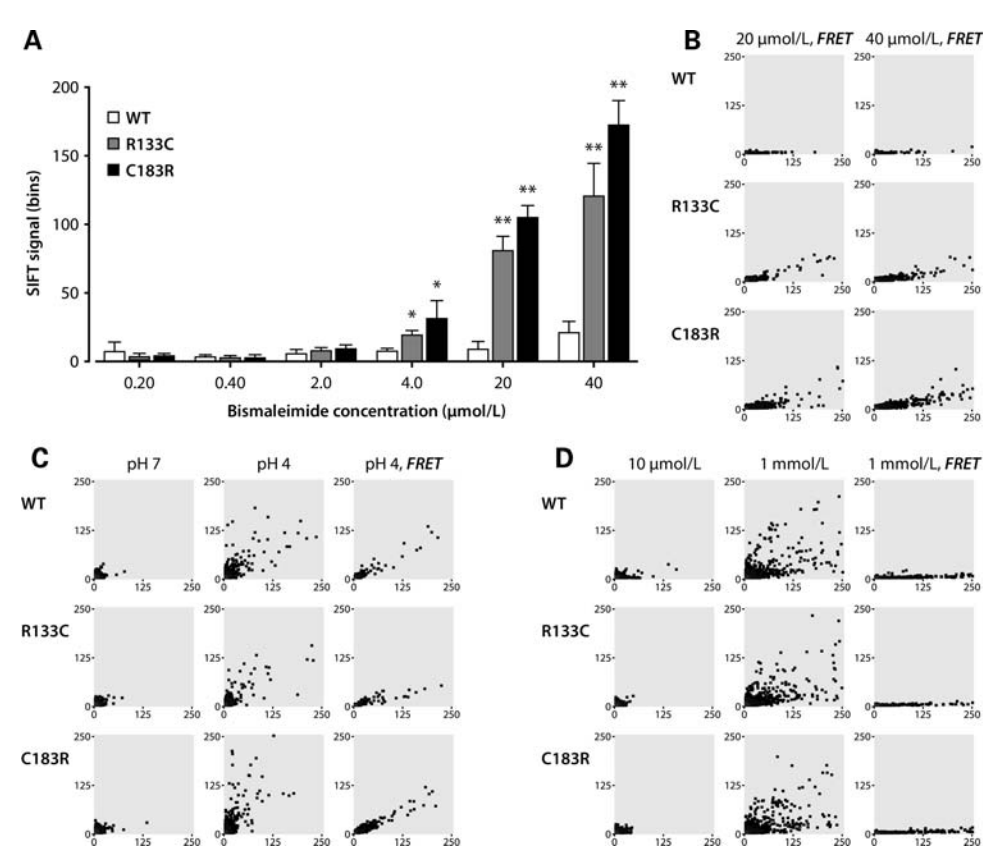


Figure 4. Crosslinking experiments with bismaleimide. (A) Quantification of dual-color high-intensity signals from SIFT analysis at increasing bismaleimide concentrations (1 h incubation). Mean + SEM of eight independent experiments (group statistics compared with WT at the same concentration;  $^*P < 0.05$ ;  $^*P < 0.01$ ; two-tailed Mann–Whitney test). SIFT panels of a representative experiment can be found in Supplementary Material, Fig. S1. (B) FRET analysis at 20 and 40  $\mu$ mol/l. (C) FRET-positive multimers induced by acidic pH can be equally detected for all N3-EGF<sub>1-5</sub> constructs providing a positive control for single-particle FRET. (D) Incubation with homocysteine promotes multimer formation. No apparent difference can be seen between WT and mutant constructs. The resulting multimers show no FRET.

other hand, the absence of FRET in homocysteine-induced multimers suggests that the multimerization mechanism is different from CADASIL-mutant aggregates which are related to unbound cysteine residues. However, the exact structural properties of N3 multimers under these conditions need to be explored in further studies.

Intriguingly, our experiments with acidic pH show that multimers generated by denaturation share FRET properties with spontaneously formed multimers. In principle, this could imply that—instead of a specific mechanism—multimerization is driven by an increased susceptibility of the mutant protein towards spontaneous denaturation. This needs to be explored in further studies.

Previous experiments with N3-EGF<sub>1-5</sub> showed dimers on SDS-PAGE under non-reducing but not under reducing conditions (23). We extend these data significantly by demonstrating spontaneous formation of higher order multimers for these constructs on non-reducing PAGE. These multimers are completely dissolved using PAGE under reducing conditions. SIFT experiments amend that reducing agents alone are not sufficient to dissolve the multimers, but the combination with an ionic detergent is required. In this regard, the multimers created in our assay closely resemble findings in autopsy material from CADASIL patients: extraction

experiments from brain tissue show that mutant N3 can only be solubilized using the above mentioned conditions.

Some technical aspects of our study need to be discussed: we used a truncated 25 kDa protein fragment of N3. Ideally, these experiments would be performed with the entire N3-ECD (210 kDa), which accumulates in CADASIL brains. However, both N3-ECD and shorter fragments comprising the first 15 EGF repeats failed to exit overexpressing cells (Fig. 1B and data not shown) most likely due to protein misfolding. Nevertheless, the EGF<sub>1-5</sub> fragment used in our study bears the mutational hot spot with 70% of all known CADASIL mutations (15). In theory, the lack of WT multimerization in our current experiments might be attributed to the truncated fragment, when assuming that multimerization of the WT depends on EGF-like repeat domains other than 1-5. Therefore, our results cannot fully exclude multimerization of full-length WT protein. However, as discussed above, even multimerization of WT N3-EGF<sub>1-5</sub> can be observed in cell lysates and is therefore most likely related to incorrectly folded protein. Nevertheless, we cannot exclude that multimerization of WT N3 in cell lysates results from an interaction of N3 with proteins from the cell lysate. In our view, the use of correctly folded protein from cell supernatants greatly outweighs the limitations.

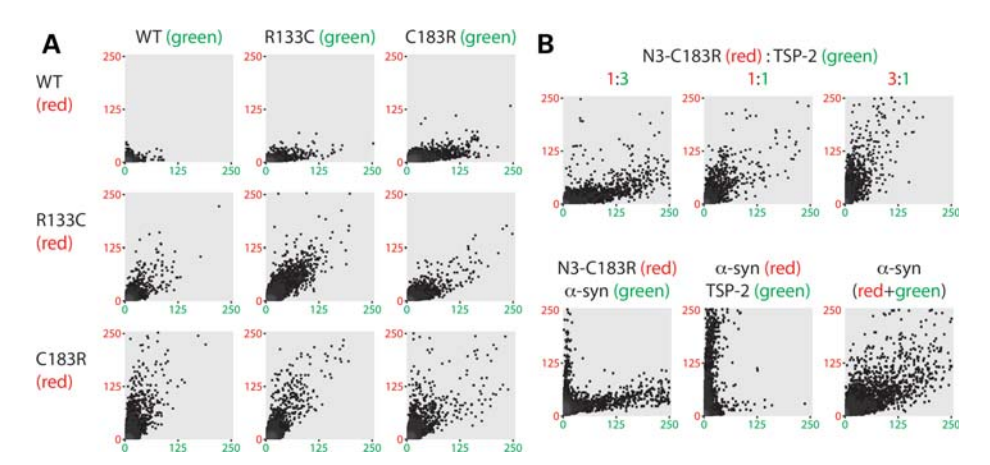


**Figure 5.** Co-aggregation of mutant N3 with WT N3 and TSP-2. (**A**) Combinations of green or red fluorescent dye-labeled WT, R133C and C183R proteins were incubated for 3 days at 37°C. (**B**) Upper panels: mixtures of TSP-2 (green labeled) and C183R-mutant N3 (red labeled), incubated for 3 days at 37°C at different molar ratios, show abundant dual-color high-intensity signals, indicating co-aggregation. Lower panels: dual-color SIFT signals from co-aggregation are absent in control experiments using alpha-synuclein (a-syn) together with C183R-mutant N3 or TSP-2. Instead, mono-colored high-intensity signals are present for a-syn and N3, originating from independent aggregation processes of these two proteins.

SIFT is an established method to study co-aggregation of proteins (24). In addition to high sensitivity, this approach offers a unique opportunity to study co-aggregation processes as the ratio of two fluorescently labeled components can be analyzed for each aggregate separately in a single assay. Therefore, the molecular composition of aggregates can be studied even in samples containing a mixture of different types of aggregates. We show for the first time that WT N3 can participate in aggregates of mutant N3. This has potentially important implications for CADASIL pathogenesis: N3 is predominantly expressed in arterial vascular smooth muscle cells and pericytes (25,26) and seems to have antiapoptotic properties (27). Apoptosis (28,29) and vascular cell degeneration (30,31) might play an important role and therefore a loss of N3 function has been discussed as a potential pathomechanism of CADASIL. Previous studies in cell culture or mouse models found no direct evidence for a classic gain or loss of receptor signaling of mutant N3 (6-8)and strongly argued for a neomorphic mechanism of CADASIL mutations (22). Sequestration of WT N3 in multimers formed by mutant N3, as suggested by our experiments, might provide such a mechanism by interfering with normal N3 receptor signaling. For example, N3 aggregates might interact with full-length N3 receptors on the cell surface, thereby altering the signaling properties, for instance through an interference with ligand binding. The observation that CADASIL-mutant N3 can rescue the developmental phenotype of N3-deficient mice (8) shows that the mutant N3 monomer enables appropriate N3 signaling. However, it does not exclude the possibility that the CADASIL phenotype, occurring later in these mice, is based on altered N3 function, when multimerization and therefore sequestration of receptors reach a critical level.

In a similar manner, sequestration of other proteins by N3 multimers might lead to altered function of these proteins. Here we show a specific participation of TSP-2, a well-known interaction partner of N3, in the aggregation process of mutant N3. Control experiments with alpha-synuclein reveal that this co-aggregation is specific. Sequestration of TSP-2 into mutant

N3 aggregates might as well disturb the N3 receptor signaling pathway, where TSP-2 is involved (20,32). Although TSP-2 is a physiological interactor of N3, binding to mutant N3 aggregates might be due to a different, neomorphic interaction mechanism. Similarly, other proteins might be trapped and thereby altered in their physiological function.

In summary, our study demonstrates that the propensity to form multimers is limited to CADASIL-mutant N3, but that WT N3 can be a component of the resulting aggregates. Our study emphasizes the need for correctly folded protein in aggregation experiments. Sequestration of other proteins, like WT N3 or TSP-2, provides a potential basis for a new pathogenic mechanism: altered function of the trapped proteins. Our robust N3 aggregation assay proved suitable for systematic analysis of the N3 multimerization process and will facilitate approaches for the screening of anti-aggregatory substances or conditions. Better understanding of N3 aggregation and co-aggregation may eventually lead to novel therapeutic strategies.

#### **MATERIALS AND METHODS**

#### Constructs

Human N3-ECD constructs have been described previously (7,14). Smaller fragments consisting of the signal peptide and EGF-like repeats 1–5 (amino acids 1–234) or 1–15 (amino acids 1–618) were created as fusion proteins with a myc-6xHIS-tag at the C-terminus: first, the coding sequence was amplified by Pfu polymerase (Stratagene, Amsterdam, the Netherlands) using a template vector containing N3-ECD and primers introducing appropriate restriction enzyme sites (*HindIII* and *XbaI*). The PCR product was cloned into pcDNA3.1(+)-mycHIS(A) (Invitrogen, Karlsruhe, Germany) in order to append the tag at the C-terminus. Second, the resulting coding sequence of the fusion protein was amplified in order to introduce restriction enzyme sites in the 5' (*Eco*RI) and 3' (*Bam*HI) untranslated regions suitable for cloning into pTT5 vector (a kind gift of Y. Durocher, National Research

Council, Quebec, Canada). The entire coding sequence of all constructs was sequenced. Plasmid maxi preparations (Hispeed Maxi Kit; QIAGEN, Hilden, Germany) from TOP10-cell (Invitrogen) cultures were used for transfection.

#### Cell culture and small-scale transfection

Human embryonic kidney 293-E (HEK293E) cells (Y. Durocher, Quebec, Canada) were propagated in Dulbecco's modified Eagle's medium (DMEM; Invitrogen) supplemented with 10% fetal bovine serum (FBS; Invitrogen) and 25  $\mu g/ml$  G418 sulfate (Merck Chemicals, Darmstadt, Germany). For small-scale transient transfection, cells were grown in six-well plates and transfected with 1.5  $\mu g$  of cDNA using 9  $\mu g$  of polyethylenimine (Polysciences Europe, Eppelheim, Germany) as described (33). Twenty-four hours after transfection, conditioned medium was collected, cells were washed and harvested in PBS and lysed with TNT lysis buffer (50 mmol/l Tris-HCl, pH 8; 200 mmol/l NaCl; 0.5% NP-40; protease inhibitor Complete EDTA-free, Roche Applied Science, Mannheim, Germany). After 20 min on ice, cell lysates were cleared by centrifugation at 16 000g for 20 min.

#### **Brain extractions**

Brains from CADASIL patients or healthy controls were obtained from a tissue library (BrainNet Germany). In 50 mm Tris-buffer (pH 7.5), 30 mg of brain tissue were homogenized using a TissueLyzer (QIAGEN) with 5 mm beads. For extraction, homogenates were treated with SDS (1% w/v) or/and bME (1% v/v) for 20 min on ice, followed by centrifugation at 16 000g for 30 min. Supernatants were collected for further analysis.

#### Protein electrophoresis and immunoblotting

PAGE of proteins and western blot analysis (semi-dry immunoblotting) were performed using standard protocols and equipment (BioRad, Munich, Germany, or Invitrogen): Laemmli loading buffer with or without bME and Tris-HCl gels or precast Tris-Bistris gradient gels (Invitrogen) were used. N3-ECD from brain extractions was detected using a monoclonal anti-N3 antibody (3G6, rat IgG2a) raised against the peptide sequence <sup>129</sup>AHGARCSVGPDGRFLCSC <sup>146</sup> of N3 and a 1:4000 dilution of HRP-labeled anti-rat secondary antibody (Dako, Hamburg, Germany). The myc-epitope was detected using a 1:4000 dilution of monoclonal mouse anti-myc 9E10 and a 1:8000 dilution of HRP-labeled anti-mouse secondary antibody (Dako), followed by chemiluminescence imaging (Immobilon Western HRP Substrate, Millipore, Schwalbach, Germany) on a Fusion-FX7 chemiluminescence system (Vilber Lourmat, Eberhardzell, Germany).

#### Large-scale expression and purification of N3-EGF<sub>1-5</sub>

A transient expression system that has been described previously (33,34) was adapted to adherent cell culture. A 500 cm² flask (Nunc/Thermo Electron LED, Langenselbold, Germany) of HEK293E cells—near confluent in DMEM with 10% FBS—was transfected with 71 μg of plasmid

DNA (pTT5-N3-EGF<sub>1-5</sub>-myc-6xHIS) and 470 μg of polyethylenimine in DMEM with 2.5% FBS. Twenty-four hours after transfection, cells were exposed to serum-free DMEM. Five days later, conditioned medium was collected, cleared from cell debris by brief centrifugation and dialyzed overnight at 4°C against PBS. Next, the dialyzed medium of four  $500 \text{ cm}^2$  flasks ( $\sim 350 \text{ ml}$ ) was incubated with 1 ml (bed volume) metal ion affinity resin (TALON, BD Biosciences Clontech, Heidelberg, Germany) for 30 min at room temperature under agitation. The resin was then transferred to a gravity-flow column and washed twice with freshly prepared wash buffer (50 mmol/l Na-phosphate, pH 7; 300 mmol/l NaCl) containing 5 mmol/l imidazole and once without imidazole. Elution was performed with PBS containing 100 mmol/l EDTA. Elution fractions were analyzed by SDS-PAGE with silver and Coomassie gel stain using standard procedures according to the manufacturer's protocols (Thermo Fisher Scientific, Bonn, Germany) or by western blot analysis as described above.

#### Fluorescent dye-labeling of proteins

N3-EGF<sub>1-5</sub> elution fractions with a purity of at least 90% were pooled and protein concentrations were determined by a Bradford assay (BioRad). One purification yielded between 100 and 300 µg of protein. The protein was concentrated and washed using a centrifugal filtration device with 3 kDa molecular weight limit (Amicon; Millipore) to a final concentration of  $\sim$ 1 mg/ml. For the labeling reaction, amino-reactive dyes Alexa Fluor® 488 or Alexa Fluor® 647 carboxylic acid succinimidyl ester (Invitrogen) were used at 3-fold molar excess. The reaction was performed overnight at 4°C in 100 mmol/l sodium bicarbonate buffer (pH 8.5). The unbound dye was removed by repeated gel filtration with spin desalting columns (Thermo Fisher Scientific) until an amount of <10% of the unbound dye was reached according to fluorescence correlation spectroscopy (FCS) autocorrelation measurements on an Insight Reader (Evotec-Technologies, Düsseldorf, Germany). Labeling efficiency was routinely checked via proteinase-K digestion to ensure equal load of fluorosphores for all constructs. Typical labeling rates were three fluorophores/molecule. With gel filtration, buffer was changed to 50 mmol/l Tris-HCl, pH 7.5, and—unless stated differently—all further incubations and reactions were performed in this buffer.

Recombinant TSP-2 (R&D Systems GmbH, Wiesbaden-Nordenstadt, Germany) was labeled with Alexa Fluor<sup>®</sup> 488 carboxylic acid succinimidyl ester (Invitrogen) accordingly. Recombinant alpha-synuclein was expressed, purified and labeled as described (35).

### Incubation experiments and confocal single-particle analysis

Incubations for spontaneous aggregation experiments were performed at a protein concentration of  ${\sim}40$  nmol/l (for the subsequent SIFT analysis) or 4  $\mu$ mol/l (for the subsequent western blot analysis) at  $37^{\circ}C$  with gentle agitation (350 r.p.m.) on a thermomixer (Eppendorf, Hamburg, Germany). For SIFT analysis at different time points,

samples were drawn and diluted 1:10 into 384-well measurement plates (Sensoplate, Greiner Bio-One, Frickenhausen, Germany), resulting in a final concentration of approximately one (green) or two (red) particles per focal volume, respectively (with the red focal volume being approximately twice as big as the green). Shorter incubation times (1 h) were used for bismaleimide (37°C), homocysteine and pH experiments (room temperature). These experiments were perin 384-well measurement formed directly Bismaleimide (1,8-bis-maleimido-diethyleneglycol; Thermo Fisher Scientific) was dissolved as 1 mmol/l stock solution in warm dH<sub>2</sub>O. For bismaleimide experiments, EDTA was added to a final concentration of 5 mmol/l to the reaction buffer and analysis was done after a short incubation of 1 h at 37°C. Homocysteine stock solution (30 mmol/l) was prepared as described (19). Reactions were incubated 1 h at room temperature. pH experiments were done in 50 mmol/l acetate (pH 4 and 5), MES (pH 6 and 7) or Tris-HCl (pH 8) buffer (all from Sigma-Aldrich, Munich, Germany).

FCS and SIFT were performed on an Insight Reader (Evotec-Technologies) with excitation laser wavelengths at 488 nm (excitation power 200  $\mu$ W) and 633 nm (300  $\mu$ W). Measurement time was 10 s with five repeats per well. Scanning parameters were set to 50 Hz beam scanner, 100  $\mu$ m scan path length and 2000  $\mu$ m positioning table movement. Data of FCS measurements were analyzed with the FCSPP evaluation software version 2.0 (Evotec-Technologies). SIFT data were recorded in two-dimensional intensity distribution histograms ( $H_{I_r,I_p}$ ) with intensity values  $I_r$ ,  $I_g$  from 0 to 255 photons/bin and bin width 40  $\mu$ s (36) and analyzed with a 2D-SIFT software module (Evotec-Technologies) as previously described (35,37).

#### Statistical analysis

Non-parametrical tests were used for group statistics: Mann—Whitney test (*U*-test, Wilcoxon rank-sum test) for independent samples and Wilcoxon signed-rank test for related samples (e.g. repeated measurements of one sample).

#### SUPPLEMENTARY MATERIAL

Supplementary Material is available at HMG online.

#### **ACKNOWLEDGEMENTS**

We thank Yves Durocher for providing HEK293E cells and pTT5 vector, and Veronika Lellek for expert technical assistance.

Conflict of Interest statement. None declared.

#### **FUNDING**

This work was supported by the Deutsche Forschungsgemeinschaft (OP 212/1-1); the Dr Werner Jackstädt-Stiftung (S 134-10.065); and the Vascular Dementia Research Foundation.

#### **REFERENCES**

- Pantoni, L. (2010) Cerebral small vessel disease: from pathogenesis and clinical characteristics to therapeutic challenges. *Lancet Neurol.*, 9, 689-701.
- Román, G.C., Erkinjuntti, T., Wallin, A., Pantoni, L. and Chui, H.C. (2002) Subcortical ischaemic vascular dementia. *Lancet Neurol.*, 1, 426–436.
- Chabriat, H., Joutel, A., Dichgans, M., Tournier-Lasserve, E. and Bousser, M.-G. (2009) CADASIL. *Lancet Neurol.*, 8, 643–653.
- Dichgans, M., Mayer, M., Uttner, I., Brüning, R., Müller-Höcker, J., Rungger, G., Ebke, M., Klockgether, T. and Gasser, T. (1998) The phenotypic spectrum of CADASIL: clinical findings in 102 cases. *Ann. Neurol.*, 44, 731–739.
- Joutel, A., Corpechot, C., Ducros, A., Vahedi, K., Chabriat, H., Mouton, P., Alamowitch, S., Domenga, V., Cécillion, M., Marechal, E. et al. (1996) Notch3 mutations in CADASIL, a hereditary adult-onset condition causing stroke and dementia. Nature, 383, 707–710.
- Joutel, A., Monet, M., Domenga, V., Riant, F. and Tournier-Lasserve, E. (2004) Pathogenic mutations associated with cerebral autosomal dominant arteriopathy with subcortical infarcts and leukoencephalopathy differently affect Jagged1 binding and Notch3 activity via the RBP/JK signaling Pathway. Am. J. Hum. Genet., 74, 338–347.
- Peters, N., Opherk, C., Zacherle, S., Capell, A., Gempel, P. and Dichgans, M. (2004) CADASIL-associated Notch3 mutations have differential effects both on ligand binding and ligand-induced Notch3 receptor signaling through RBP-Jk. Exp. Cell Res., 299, 454–464.
- Monet, M., Domenga, V., Lemaire, B., Souilhol, C., Langa, F., Babinet, C., Gridley, T., Tournier-Lasserve, E., Cohen-Tannoudji, M. and Joutel, A. (2007) The archetypal R90C CADASIL-NOTCH3 mutation retains NOTCH3 function in vivo. Hum. Mol. Genet., 16, 982–992.
- 9. Monet-Leprêtre, M., Bardot, B., Lemaire, B., Domenga, V., Godin, O., Dichgans, M., Tournier-Lasserve, E., Cohen-Tannoudji, M., Chabriat, H. and Joutel, A. (2009) Distinct phenotypic and functional features of CADASIL mutations in the Notch3 ligand binding domain. *Brain*, 132, 1601–1612.
- Downing, A.K., Knott, V., Werner, J.M., Cardy, C.M., Campbell, I.D. and Handford, P.A. (1996) Solution structure of a pair of calcium-binding epidermal growth factor-like domains: implications for the Marfan syndrome and other genetic disorders. *Cell*, 85, 597–605.
- Joutel, A., Vahedi, K., Corpechot, C., Troesch, A., Chabriat, H., Vayssière, C., Cruaud, C., Maciazek, J., Weissenbach, J., Bousser, M.G. et al. (1997) Strong clustering and stereotyped nature of Notch3 mutations in CADASIL patients. *Lancet*, 350, 1511–1515.
- Joutel, A., Andreux, F., Gaulis, S., Domenga, V., Cecillon, M., Battail, N., Piga, N., Chapon, F., Godfrain, C. and Tournier-Lasserve, E. (2000) The ectodomain of the Notch3 receptor accumulates within the cerebrovasculature of CADASIL patients. J. Clin. Invest., 105, 597–605.
- 13. Joutel, A., Monet-Leprêtre, M., Gosele, C., Baron-Menguy, C., Hammes, A., Schmidt, S., Lemaire-Carrette, B., Domenga, V., Schedl, A., Lacombe, P. et al. (2010) Cerebrovascular dysfunction and microcirculation rarefaction precede white matter lesions in a mouse genetic model of cerebral ischemic small vessel disease. J. Clin. Invest., 120, 433–445.
- Opherk, C., Duering, M., Peters, N., Karpinska, A., Rosner, S., Schneider, E., Bader, B., Giese, A. and Dichgans, M. (2009) CADASIL mutations enhance spontaneous multimerization of NOTCH3. *Hum. Mol. Genet.*, 18, 2761–2767.
- Peters, N., Opherk, C., Bergmann, T., Castro, M., Herzog, J. and Dichgans, M. (2005) Spectrum of mutations in biopsy-proven CADASIL: implications for diagnostic strategies. *Arch. Neurol.*, 62, 1091–1094.
- Behrends, C., Langer, C.A., Boteva, R., Böttcher, U.M., Stemp, M.J., Schaffar, G., Rao, B.V., Giese, A., Kretzschmar, H., Siegers, K. et al. (2006) Chaperonin TRiC promotes the assembly of polyQ expansion proteins into nontoxic oligomers. Mol. Cell, 23, 887–897.
- Lim, C.J. and Shen, W.C. (2004) Transferrin-oligomers as potential carriers in anticancer drug delivery. *Pharm. Res.*, 21, 1985–1992.
- Millonig, R., Salvo, H. and Aebi, U. (1988) Probing actin polymerization by intermolecular cross-linking. J. Cell. Biol., 106, 785–796.
- Hubmacher, D., Tiedemann, K., Bartels, R., Brinckmann, J., Vollbrandt, T., Batge, B., Notbohm, H. and Reinhardt, D.P. (2005) Modification of the structure and function of fibrillin-1 by homocysteine suggests a potential pathogenetic mechanism in homocystinuria. *J. Biol. Chem.*, 280, 34946– 34955.

- Meng, H., Zhang, X., Hankenson, K.D. and Wang, M.M. (2009) Thrombospondin 2 potentiates notch3/jagged1 signaling. *J. Biol. Chem.*, 284, 7866–7874.
- Karlström, H., Beatus, P., Dannaeus, K., Chapman, G., Lendahl, U. and Lundkvist, J. (2002) A CADASIL-mutated Notch 3 receptor exhibits impaired intracellular trafficking and maturation but normal ligand-induced signaling. *Proc. Natl Acad. Sci. USA*, 99, 17119–17124.
- Takahashi, K., Adachi, K., Yoshizaki, K., Kunimoto, S., Kalaria, R.N. and Watanabe, A. (2010) Mutations in NOTCH3 cause the formation and retention of aggregates in the endoplasmic reticulum, leading to impaired cell proliferation. *Hum. Mol. Genet.*, 19, 79–89.
- Arboleda-Velasquez, J.F., Rampal, R., Fung, E., Darland, D.C., Liu, M., Martinez, M.C., Donahue, C.P., Navarro-Gonzalez, M.F., Libby, P., D'Amore, P.A. et al. (2005) CADASIL mutations impair Notch3 glycosylation by Fringe. Hum. Mol. Genet., 14, 1631–1639.
- Giese, A., Bader, B., Bieschke, J., Schaffar, G., Odoy, S., Kahle, P.J., Haass, C. and Kretzschmar, H. (2005) Single particle detection and characterization of synuclein co-aggregation. *Biochem. Biophys. Res. Commun.*, 333, 1202–1210.
- Claxton, S. and Fruttiger, M. (2004) Periodic Delta-like 4 expression in developing retinal arteries. Gene Expr. Patterns, 5, 123–127.
- Villa, N., Walker, L., Lindsell, C.E., Gasson, J., Iruela-Arispe, M.L. and Weinmaster, G. (2001) Vascular expression of Notch pathway receptors and ligands is restricted to arterial vessels. *Mech. Dev.*, 108, 161–164.
- Wang, W., Prince, C.Z., Mou, Y. and Pollman, M.J. (2002) Notch3 signaling in vascular smooth muscle cells induces c-FLIP expression via ERK/MAPK activation. Resistance to Fas ligand-induced apoptosis.
   J. Biol. Chem., 277, 21723–21729.
- 28. Formichi, P., Radi, E., Battisti, C., Di Maio, G., Tarquini, E., Leonini, A., Di Stefano, A., Dotti, M.T. and Federico, A. (2009) Apoptosis in CADASIL: an *in vitro* study of lymphocytes and fibroblasts from a cohort of Italian patients. *J. Cell. Physiol.*, 219, 494–502.

- Viswanathan, A., Gray, F., Bousser, M.-G., Baudrimont, M. and Chabriat, H. (2006) Cortical neuronal apoptosis in CADASIL. Stroke, 37, 2690–2695.
- Lewandowska, E., Szpak, G.M., Wierzba-Bobrowicz, T., Modzelewska, J., Stepień, T., Pasennik, E., Schmidt-Sidor, B. and Rafałowska, J. (2010) Capillary vessel wall in CADASIL angiopathy. Folia Neuropathol., 48, 104–115.
- Ruchoux, M.M., Domenga, V., Brulin, P., Maciazek, J., Limol, S., Tournier-Lasserve, E. and Joutel, A. (2003) Transgenic mice expressing mutant Notch3 develop vascular alterations characteristic of cerebral autosomal dominant arteriopathy with subcortical infarcts and leukoencephalopathy. *Am. J. Pathol.*, 162, 329–342.
- 32. Meng, H., Zhang, X., Lee, S.J., Strickland, D.K., Lawrence, D.A. and Wang, M.M. (2010) Low density lipoprotein receptor-related protein-1 (LRP1) regulates thrombospondin-2 (TSP2) enhancement of Notch3 signaling. *J. Biol. Chem.*, **285**, 23047–23055.
- Pham, P.L., Kamen, A. and Durocher, Y. (2006) Large-scale transfection of mammalian cells for the fast production of recombinant protein. *Mol. Biotechnol.*, 34, 225–237.
- Durocher, Y., Perret, S. and Kamen, A. (2002) High-level and high-throughput recombinant protein production by transient transfection of suspension-growing human 293-EBNA1 cells. *Nucleic Acids Res.*, 30, E9.
- Kostka, M., Hogen, T., Danzer, K.M., Levin, J., Habeck, M., Wirth, A., Wagner, R., Glabe, C.G., Finger, S., Heinzelmann, U. *et al.* (2008) Single particle characterization of iron-induced pore-forming alpha-synuclein oligomers. *J. Biol. Chem.*, 283, 10992–11003.
- Bieschke, J., Giese, A., Schulz-Schaeffer, W., Zerr, I., Poser, S., Eigen, M. and Kretzschmar, H. (2000) Ultrasensitive detection of pathological prion protein aggregates by dual-color scanning for intensely fluorescent targets. *Proc. Natl Acad. Sci. USA*, 97, 5468–5473.
- Levin, J., Bertsch, U., Kretzschmar, H. and Giese, A. (2005) Single particle analysis of manganese-induced prion protein aggregates. *Biochem. Biophys. Res. Commun.*, 329, 1200–1207.